Molecular Systems Biology 9; Article number 636; doi:10.1038/msb.2012.71
Citation: ***Molecular Systems Biology*** **9:636**
www.molecularsystemsbiology.com

molecular systems biology

Autonomous bacterial localization and gene expression based on nearby cell receptor density

Hsuan-Chen Wu[1,2], Chen-Yu Tsao[1,2], David N Quan[1,2], Yi Cheng[3], Matthew D Servinsky[4], Karen K Carter[2,5], Kathleen J Jee[1], Jessica L Terrell[1,2], Amin Zargar[2,5], Gary W Rubloff[3], Gregory F Payne[1,2], James J Valdes[6] and William E Bentley[1,2,5,*]

[1] Fischell Department of Bioengineering, University of Maryland, College Park, MD, USA, [2] Institute for Bioscience and Biotechnology Research, University of Maryland, College Park, MD, USA, [3] Department of Material Science and Engineering, University of Maryland, College Park, MD, USA, [4] Sensors and Electron Devices Directorate, US Army Research Laboratory, Adelphi, MD, USA, [5] Department of Chemical and Biomolecular Engineering, University of Maryland, College Park, MD, USA and [6] US Army Edgewood Chemical Biological Center, Aberdeen Proving Ground, MD, USA
* Corresponding author. Institute for Bioscience and Biotechnology Research, University of Maryland, 5115 Plant Sciences Building, College Park, MD 20742, USA. Tel.: +1 301 405 4321; Fax: +1 301 405 9953; E-mail: bentley@umd.edu

Received 16.7.12; accepted 8.12.12

Escherichia coli **were genetically modified to enable programmed motility, sensing, and actuation based on the density of features on nearby surfaces. Then, based on calculated feature density, these cells expressed marker proteins to indicate phenotypic response. Specifically, site-specific synthesis of bacterial quorum sensing autoinducer-2 (AI-2) is used to initiate and recruit motile cells. In our model system, we rewired *E. coli's* AI-2 signaling pathway to direct bacteria to a squamous cancer cell line of head and neck (SCCHN), where they initiate synthesis of a reporter (drug surrogate) based on a threshold density of epidermal growth factor receptor (EGFR). This represents a new type of controller for targeted drug delivery as actuation (synthesis and delivery) depends on a receptor density marking the diseased cell. The ability to survey local surfaces and initiate gene expression based on feature density represents a new area-based switch in synthetic biology that will find use beyond the proposed cancer model here.**

Molecular Systems Biology **9:** 636; published online 22 January 2013; doi:10.1038/msb.2012.71
Subject Categories: synthetic biology; metabolic and regulatory networks
Keywords: cancer; EGFR; *Escherichia coli*; quorum sensing; synthetic biology

Introduction

Synthetic biology engenders design-based rewiring of a cell's genetic circuitry for the synthesis of novel products (Kwok, 2010). In such cases, cell populations are aligned for optimal production. While Nature's biosynthetic toolbox is vast—missing are measures that exploit high level functions of cells to enable autonomously computed and directed outcomes (Tsao *et al*, 2010). That is, a less commonly examined but equally innovative strategy envisions a reprogrammed cell itself or small collections of cells as the end products of synthetic biology, as these cells execute extraordinary tasks (Forbes, 2010). Recently, Saeidi *et al* (2011) engineered an *E. coli* to sense and kill nearby pathogenic *P. aeruginosa* by secreting pyocin S5 in response to its identifying signal molecule, $3OC_{12}HSL$. Indeed, engineered signaling or communication networks are envisioned to endow bacteria with the ability to seek out new populations (Defoirdt, 2011). Bacteria have also been engineered to carry and deploy 'cargo' at selected surfaces (Fernandes *et al*, 2011). These concepts have yet to be combined for autonomous operation.

Bacteria harness the signal transduction processes of quorum sensing (QS) as a means of inter- and intra-species communication and the coordination of population-based phenotypes. This cell-to-cell communications network is controlled by the synthesis, transport, and sensing of its autoinducer signaling molecules. Contrary to the idea that it is the cell number that initiates a QS response, several studies have demonstrated that autoinducer concentration is the determining factor. That is, by manipulating the autoinducer concentration via genetic, physical, or biochemical means, one can elicit a QS response in even one (Carnes *et al*, 2010) or a few bacterial cells (Fernandes *et al*, 2010). For example, we created an autoinducer-2 (AI-2) synthesizing fusion protein (referred to as a 'nanofactory') onto which any antigen-targeting antibody can be assembled for antigen-localized AI-2 synthesis (Fernandes *et al*, 2010). This was used to elicit a QS response among one strain from within a mixed culture of two AI-2 responding strains and in the absence of a quorum.

By altering their QS genetic circuits, we engineered bacteria to find cells of interest (diseased or otherwise), dock on associated surface receptors or biomarkers ('features'), integrate surface feature density, and also decide whether or not to initiate gene expression. This 'smart' bacterium reinforces the notion of an expanded synthetic biology umbrella that confers new capabilities on the individual cell. The resultant cell has capabilities that could be viewed as analogous to a dirigible—a transport vehicle that autonomously navigates and carries or deploys important cargo.

Report Documentation Page

Form Approved
OMB No. 0704-0188

1. REPORT DATE	2. REPORT TYPE	3. DATES COVERED
22 JAN 2013		**00-00-2013 to 00-00-2013**

4. TITLE AND SUBTITLE	5a. CONTRACT NUMBER
Autonomous bacterial localization and gene expression based on nearby cell receptor density	5b. GRANT NUMBER
	5c. PROGRAM ELEMENT NUMBER
6. AUTHOR(S)	5d. PROJECT NUMBER
	5e. TASK NUMBER
	5f. WORK UNIT NUMBER
7. PERFORMING ORGANIZATION NAME(S) AND ADDRESS(ES) **US Army Research Laboratory,Sensors and Electron Devices Directorate,Adelphi,MD,20783**	8. PERFORMING ORGANIZATION REPORT NUMBER
9. SPONSORING/MONITORING AGENCY NAME(S) AND ADDRESS(ES)	10. SPONSOR/MONITOR'S ACRONYM(S)
	11. SPONSOR/MONITOR'S REPORT NUMBER(S)

12. DISTRIBUTION/AVAILABILITY STATEMENT
Approved for public release; distribution unlimited

13. SUPPLEMENTARY NOTES
Molecular Systems Biology 9:636, Published online 22 January 2013

14. ABSTRACT

Escherichia coli were genetically modified to enable programmed motility, sensing, and actuation based on the density of features on nearby surfaces. Then, based on calculated feature density, these cells expressed marker proteins to indicate phenotypic response. Specifically, site-specific synthesis of bacterial quorum sensing autoinducer-2 (AI-2) is used to initiate and recruit motile cells. In our model system, we rewired E. coli?s AI-2 signaling pathway to direct bacteria to a squamous cancer cell line of head and neck (SCCHN), where they initiate synthesis of a reporter (drug surrogate) based on a threshold density of epidermal growth factor receptor (EGFR). This represents a newtype of controller for targeted drug delivery as actuation (synthesis and delivery) depends on a receptor density marking the diseased cell. The ability to survey local surfaces and initiate gene expression based on feature density represents a new area-based switch in synthetic biology that will find use beyond the proposed cancer model here.

15. SUBJECT TERMS

16. SECURITY CLASSIFICATION OF:			17. LIMITATION OF ABSTRACT	18. NUMBER OF PAGES	19a. NAME OF RESPONSIBLE PERSON
a. REPORT **unclassified**	b. ABSTRACT **unclassified**	c. THIS PAGE **unclassified**	**Same as Report (SAR)**	**9**	

The particular circumstances of our exploratory experiments leveraged the AI-2 signaling pathway of bacterial QS to direct bacterial swimming to a squamous cancer cell line of the head and neck (SCCHN) and subsequently initiate the synthesis of a reporter protein based on a threshold density of epidermal growth factor receptor (EGFR). Several studies have demonstrated the use of bacteria for both the synthesis and delivery of proteins or other toxins in cancer models (Forbes, 2010). None, however, have demonstrated high level discrimination of tumor from healthy cells with regard to differential surface biomarker profiles. In our case, cell localization was also governed by bacterial chemotaxis, since AI-2 is a chemoattractant, recruiting bacteria to its place of synthesis. Bacterial swimming was thus initiated and guided by site-directed synthesis and diffusion of AI-2 from a template-assembled nanofactory. AI-2 is a chemoattractant and serves as a molecular sentinel that recruits bacteria to its place of synthesis. Upon arrival, the bacteria sensed the prevailing AI-2 concentration that was directly proportional to the local EGFR surface density. A pre-programmed QS response then served to coordinate phenotype by initiating DsRed gene expression within the localized population of bacteria. Overall, this serves as a phenotype 'focusing' system (Balazsi *et al*, 2011; Xie *et al*, 2011) and maintains the switch in an 'off' state until the desired threshold is reached (Figure 1).

Results

AI-2 synthesis from template-assembled nanofactories and activation of docked bacteria

In Figure 1, the bacterium's motility and switching capabilities rely upon bacterial QS, a density-dependent cell–cell communication process mediated by the transmission and propagation of chemical autoinducers (Miller and Bassler, 2001; Waters and Bassler, 2005). Responding to a threshold autoinducer level coincident with a quorum, cells initiate coordinated changes in gene expression (Hooshangi and Bentley, 2008). Recognizing the complexities of this system that arise from its chemical reaction, diffusion, cell motility, and gene expression components, we first constructed a series of studies using biofabricated surfaces that enabled spatio-temporally controlled microenvironments for elucidating design and fabrication parameters. Receptor and signaling gradients were assembled via avidin-loaded biotin-coated ELISA wells. In Figure 2A, avidin is a target for FITC-labeled rabbit anti-avidin IgG conjugated AI-2 synthesizing nanofactories (NFs) (Fernandes *et al*, 2010). The NF is a chimeric fusion protein expressed and purified from *E. coli* consisting of an IgG-binding motif (protein G), two AI-2 synthases, Pfs and LuxS, which convert S-adenosylhomocysteine (SAH) into AI-2, and affinity tags for covalent or metal-ion coupling to surfaces. In Figure 2B, we depict the level of NF binding and AI-2 production as a function of coated avidin. We used a mathematical model for *E. coli's* AI-2 regulated QS genetic switch (Hooshangi and Bentley, 2011) to evaluate sensitivity and strength of the switch as a function of ambient AI-2 concentration. Correspondingly, we engineered *E. coli* (W3110 Δ*lsrFG* Δ*luxS*) for hypersensitivity to AI-2 and inoculated them into wells above the NF. Upon detection of ~1–5 μM AI-2, these cells express T7 polymerase that amplifies the native *lsr* operon response by overexpressing DsRed (see Supplementary Figure 1). NF fluorescence, AI-2 level, and DsRed production from these AI-2 responding cells were all correlated, as expected. NF was bound to the surface with saturation dependence (e.g., Langmuir isotherm). AI-2 levels were proportional to NF loading. DsRed profiles indicate both that: (i) cells responded proportionally to the AI-2 level and (ii) AI-2 concentration increased monotonically over the 26-h owing to sustained Pfs and LuxS enzymatic activity as assembled on chips. Results from Figures 2A to C demonstrate binding of the signal-generating NF to a programmed feature-ladened surface through antigen–antibody interaction. This enabled calibration of both AI-2 productivity and the AI-2 cell response.

A functioning system requires autonomously triggered gene expression of bacterial cells that are immediately proximal or in direct contact with surface features. To design and test this attribute, we engineered bacteria so they would 'dock' onto surfaces. In Supplementary Figure 2, we expressed *Streptococcal* protein G (Tanaka *et al*, 2006) as a surface-displayed

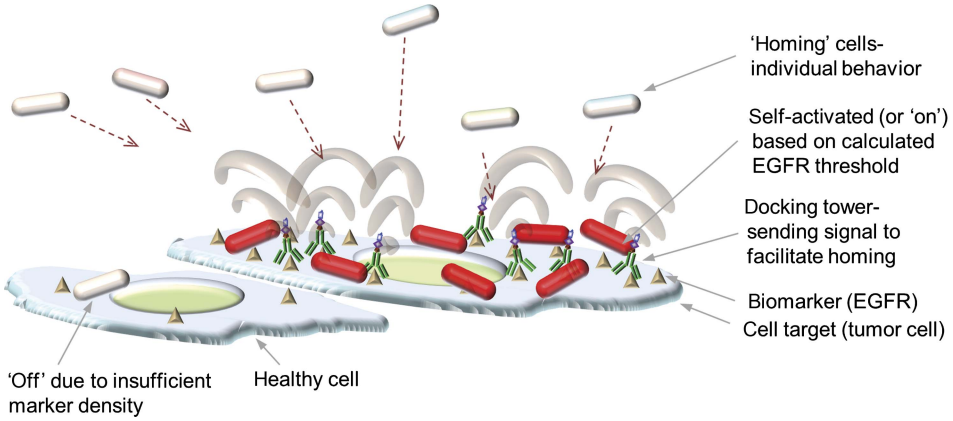

Figure 1 A bacterial 'dirigible' concept. Biological nanofactories (NFs) that synthesize bacterial AI-2 are targeted to epidermal growth factor receptor (EGFR) on the surface of squamous cell carcinoma of head and neck (SCCHN) line, PCI-15B. AI-2 molecules are emitted from the cell surface and recognized by reprogrammed bacteria, which swim to the site of signal generation and decide, based on AI-2 level (which is proportional to the EGFR surface density), whether or not to initiate gene expression.

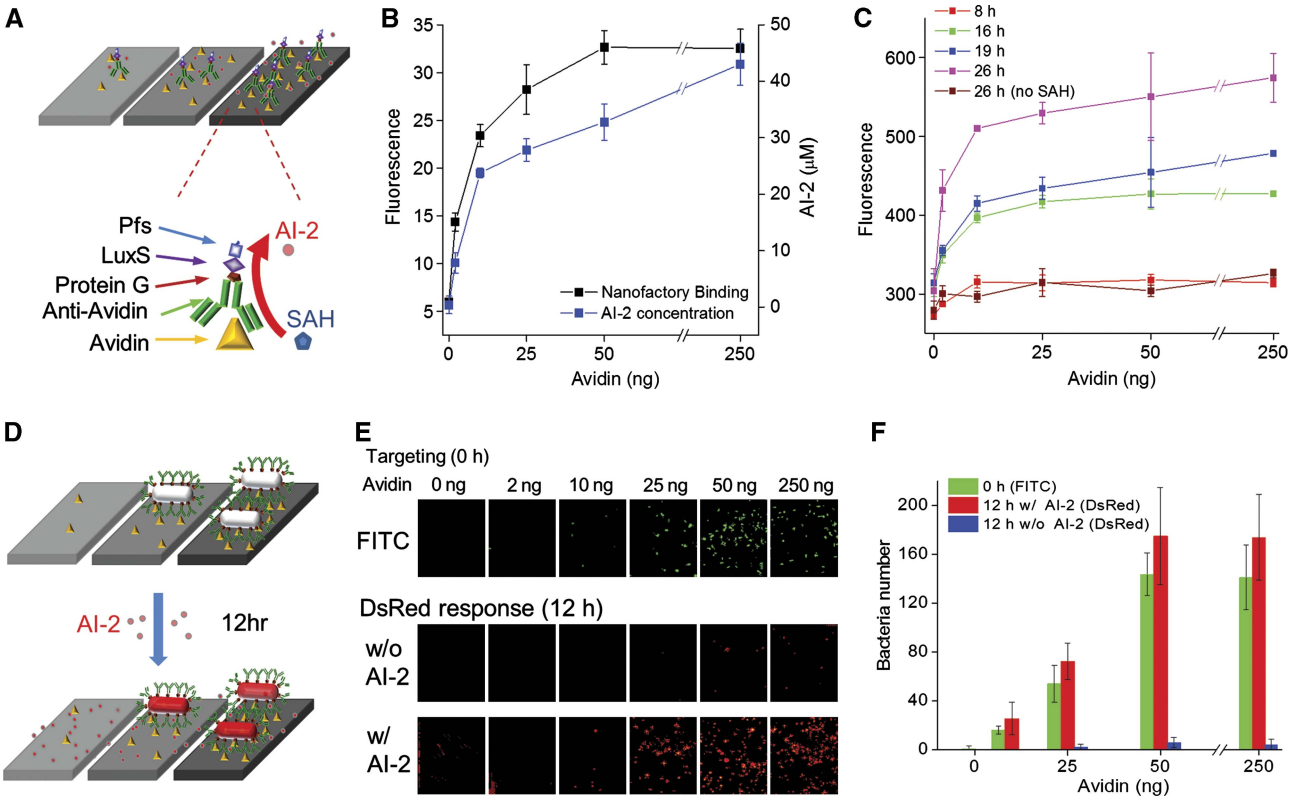

Figure 2 *In situ* generation of AI-2 though surface assembled NF and QS-activated gene expression from 'docked' bacterial cells. (**A**) Scheme for NF targeting on various densities of avidin chips. NFs are fusion proteins comprising Pfs, LuxS (for AI-2 synthesis) and protein G (IgG-binding motif, for antibody conjugation). Anti-avidin (FITC) coupled NFs target to avidin-coated chips and catalyze SAH to AI-2. (**B**) NF targeting and subsequent *in vitro* AI-2 synthesis on avidin plate wells. NF loading was determined by FITC fluorescence and AI-2 concentrations were measured by Ellman's assay (Fernandes *et al*, 2010). (**C**) *E. coli* W3110 (Δ*lsrFG* Δ*luxS*) response to *in vitro* AI-2 synthesized by NF assembled onto avidin plate wells. Bacterial suspensions were added directly to wells and DsRed intensities were measured via fluorescence plate reader. The negative control is without SAH addition. (**D**) Conceptual bacterial docking via surface-expressed protein G and outer membrane assembled anti-avidin IgG facilitating binding to avidin on chip surface. Subsequent application of AI-2 triggers QS switch (*lsr* gene expression) as indicated by DsRed fluorescence. (**E**) *E. coli* W3110 cells with surface-expressed protein G decorated with anti-avidin IgG were applied to wells with various avidin densities. Unbound bacteria were washed followed by 40 μM AI-2 addition (this concentration is above QS threshold). After 12 h, fluorescence images depict immobilized cells. (**F**) Image analysis (ImageJ) revealed number of bacteria on avidin surfaces. Both cell number and DsRed fluorescence were linear with avidin loading. Source data for this figure is available on the online supplementary information page.

fusion with outer membrane protein A (OmpA vector provided by Dr Georgiou; Francisco *et al*, 1992) in W3110 (Δ*lsrFG* Δ*luxS*). This allowed *ex vivo* assembly of antibody for targeting and docking *E. coli* to any specified surface. Exactly analogous to NF assembly (Figure 2A), anti-avidin IgG-coated bacteria were loaded onto avidin-coated chips (Figure 2D) and incubated with 40 μM AI-2. The number of bound FITC-labeled bacteria increased linearly with avidin until 50 ng (Figures 2E and F). Correspondingly, the number of AI-2 responding cells also increased linearly, demonstrating that AI-2 sensing bacterial cells were spatially organized on antigen-laden surfaces in proportion to feature density.

QS activation of docked bacteria on PCI-15B via EGFR

In Figure 3A, we identically reformulated these immobilization protocols using SCCHN, PCI-15B (Thomas *et al*, 2004) (provided by Dr Grandis) that displays EGFR at high levels (Wheeler *et al*, 2010; Sahu and Grandis, 2011). We used HEK293 (human embryonic kidney cells) for healthy cell controls (low expression of EGFR). Both were seeded in 96-well plates of increasing cell density (also receptor density). *E. coli* cells were induced with 0.5 mM IPTG for 2 h to express OmpA:protein G followed by coupling of AF488-labeled mouse anti-EGFR IgG (denoted as anti-EGFR). Bacterial cells were then cultivated with PCI-15B and HEK293 cells for EGFR targeting. After 0.5 h, the wells were washed with DPBS to rinse off unbound bacteria and treated with goat anti-mouse coupled NF (Figure 3A). Thus, AI-2 synthesized should be proportional to surface feature density (via linearity between cell number and surface receptor density); also those bacterial cells directly in contact would be exposed to AI-2. After washing with DPBS, an SAH solution was added and bacterial fluorescence was monitored. In Figures 3B and C, fluorescent and bright field images indicate that the anti-EGFR bacteria were bound to the cell surfaces. Moreover, there was a linear increase in bound bacteria with eukaryotic cell number until 10 000/well ($R^2 = 0.97$). Importantly, after 12 h with SAH, bacterial cells at only the two highest mammalian seeding densities (10 000 and 20 000 cells/well) exhibited DsRed expression indicating the QS switch was 'on'. Wells with low PCI-15B densities or without NF treatment had minimal DsRed

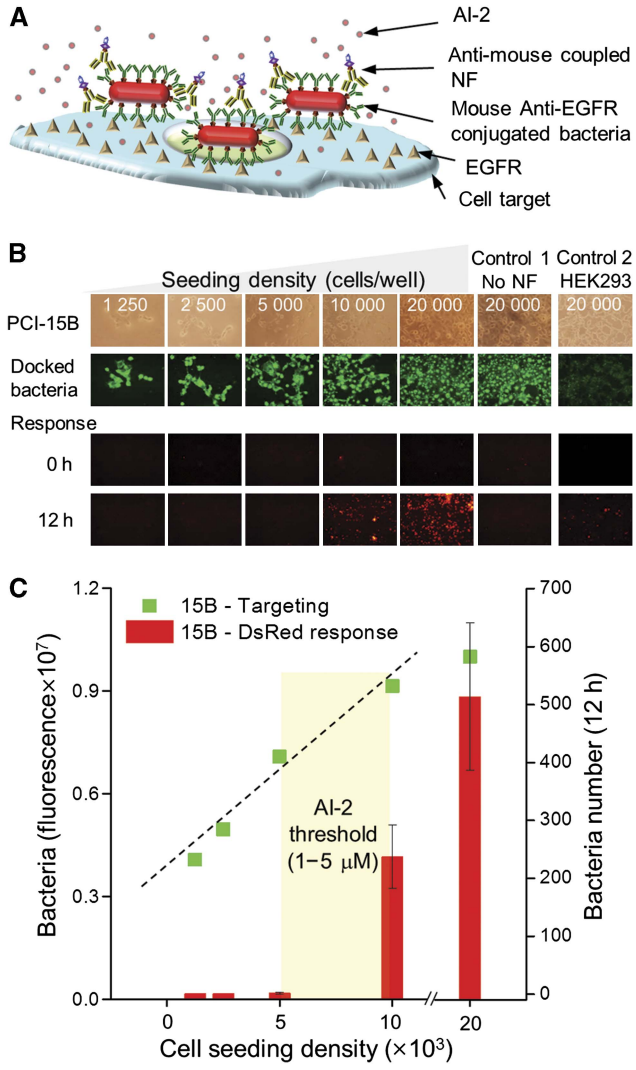

Figure 3 *E. coli* targeted to SCCHN cell line PCI-15B via EGFR and QS activation of gene expression. (**A**) Scheme for targeting and docking bacteria to receptors on mammalian cell surfaces and subsequent NF conjugation to targeted bacteria for local AI-2 synthesis and delivery bacteria for triggering QS switch. The protocol follows: (i) anti-EGFR IgG decorated bacteria facilitate cell binding to EGFR on PCI-15B cell surfaces; (ii) secondary Ab-NFs are directed to immobilized bacteria; and (iii) NFs convert SAH into AI-2 for initiating gene expression (*lsr* operon). (**B**) Indicated densities of PCI-15B or HEK293 cells were seeded to wells followed by mouse anti-EGFR (AF488-labeled) bacteria, anti-mouse-NF targeting and subsequent SAH addition. DsRed expression was measured after 12 h. (**C**) Analyses of fluorescent images yielded linear increase in both cell number and DsRed fluorescing cells with PCI-15B loading (reflective of EGFR density). The HEK293 control sample exhibited 3.4×10^6 AF488 fluorescence, which indicates bacterial docking ~1/3 that of PCI-15B at seeding density of 20 000 cells/well. Source data for this figure is available on the online supplementary information page.

expression, similar to the HEK293 control cell surface. These data demonstrate successful QS-directed switching for surface bound cells and that the resultant threshold limit for initiating gene expression was directly related to EGFR density. Based on previous work (Fernandes *et al*, 2010) and these data, we estimate 410 bacteria responded to $0.5–2.4 \times 10^9$ EGFRs in a 1-mm^2 area. This corresponds to $\sim 0.15–0.75 \times 10^6$ EGFRs per cell that falls within the anticipated range (Zimmermann *et al*, 2006).

AI-2 attracts bacteria

Next, to establish directed bacterial motility we exploited recently discovered AI-2-mediated chemotaxis (Hegde *et al*, 2011). That is, we created a defined AI-2 gradient as a stimulus for evaluating *E. coli* motility. A conventional drug-delivery transwell plate apparatus was loaded with 40 μM AI-2 in the upper chamber and W3110 bacteria in the lower chamber; samples from each were withdrawn after 1 and 2 h. In Figure 4A, the calculated concentration gradient is depicted at different regions in the transwell apparatus. While the geometry of the system makes somewhat obscure the exact gradient experienced by each bacterium, the 'typical' cell as determined by the relative area within the apparatus will be exposed to gradients depicted at points C and D where the gradient is largely dissipated after 20 min. Figures 4B and C demonstrate that one-third of the bacteria originally placed in the lower chamber had swum vertically against gravity into the upper chamber. In the transwell apparatus, we found the bacteria typically needed >1 h to respond and swim the estimated 3.5 mm distance. Subsequent analysis (Supplementary Figures 3–5) showed that at a gradient as small as 0.06 mM/mm was needed to elicit a rapid motility response from sessile *E. coli*. In a controlled microfluidic device with directionally defined AI-2 gradient, we found the preponderance of bacteria could swim a 0.5-mm distance within 30–40 min.

Functioning programmed system

Results from Figures 1 to 4 demonstrate that time and concentration domains must be known and integrated into a functional system design. In Figure 5, we depict the assembled system comprising motile and sensing/actuating bacteria that (i) detect signal molecules emanating from receptors on tumor cells, (ii) migrate to the tumor cells, and (iii) based on receptor density, initiate gene expression. Recognizing that genome reconstruction in synthetic biology may have metabolic consequences that interfere with programmed function (Bentley *et al*, 1990; DeLisa *et al*, 2001; Kwok, 2010), our design comprising only minimally rewired genetic circuits (Tsao *et al*, 2010). In Figure 5A, we seeded mammalian PCI-15B and HEK293 cells on gelatin-coated glass coverslips, introduced anti-EGFR-NF complexes onto confluent cell layers, and applied SAH (500 μM) into the top compartment of a transwell apparatus. We then turned the gelatin coverslips upside-down allowing direct vertical streamlines from bacteria to mammalian cells. The W3110 (Δ*lsrFG* Δ*luxS*) cells were added to the lower wells and after a 9-h incubation (time sufficient for AI-2 synthesis, gradient formation, bacterial migration, and bacterial gene expression) we checked whether the bacteria had successfully migrated upwards to the targeted mammalian surfaces and initiated gene expression. We measured bacterial OD, *in vitro* AI-2 concentration, bound NF (AF488-labeled anti-EGFR), and also DsRed fluorescence after mammalian cells had been washed off unattached bacteria and NF (Figures 5B and C). The number of bacteria found in the upper chamber was highest for the PCI-15B cells treated with SAH, in accordance with the higher level of AI-2. The levels of AI-2 observed in the upper chamber were ~5 μM

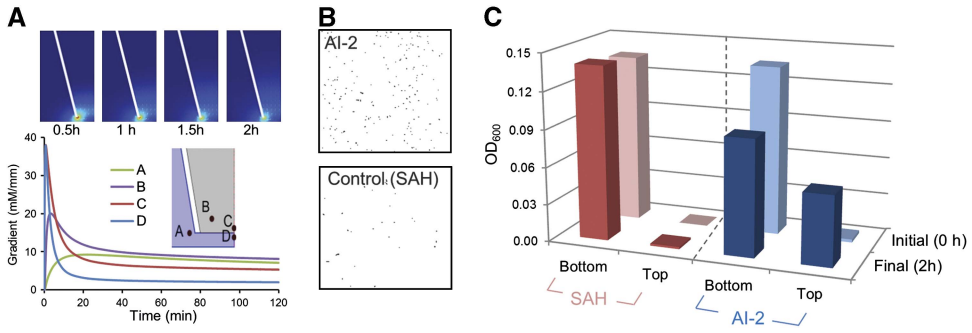

Figure 4 Bacterial motility directed to AI-2. (**A**) Simulation (COMSOL) of AI-2 concentration profile over time within the transwell apparatus. AI-2 was loaded in the upper chamber where it could diffuse through the membrane to the lower chamber (initially buffer). The top four plots represent the concentration gradients in time. The bottom chart depicts the dynamics of the local concentration gradient at specific sites (A, B, C, and D). Chemotaxis experiments were performed as follows: 40 μM AI-2 or SAH (control) was added to the upper chamber of the 3 μm 6-well inserts. W3110 cells (OD ~1–1.5) rinsed with DPBS three times were then resuspended into DPBS (OD ~0.14) and applied into bottom wells. The inserts were incubated under static conditions at 37 °C for 2 h. Samples were obtained from each chamber via pipette. (**B**) Determination of bacterial migration under bright field microscopy. (**C**) Systematic optical density measurements (OD_{600}) were conducted to assess migration from the source (bottom) upward toward the chemoattractant (top). Source data for this figure is available on the online supplementary information page.

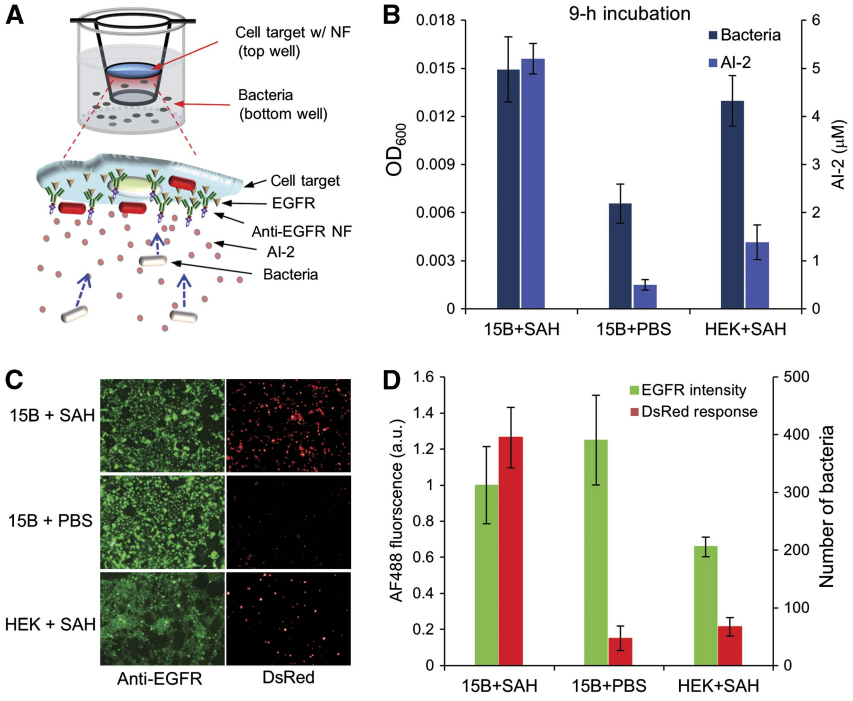

Figure 5 Autonomously functioning sense and respond system. (**A**) Schematic depicts nanofactories assembled onto EGFRs on surface of PCI-15B cells. These cells, in turn, are cultivated on an inverted transwell insert exposing cell surfaces and nanofactories to the bacterial cells initially seeded on the bottom of the transwell apparatus. The bacteria then migrate vertically toward mammalian cells and subsequently initiate gene expression by sensing the *in vitro* AI-2 gradient, which is locally synthesized by the NF located on the mammalian cell surfaces. (**B**) After 9 h, bacteria and AI-2 levels were assayed in the upper chamber. (**C**) PCI-15B cells were rinsed and both QS-activated bacteria (DsRed) and NF (AF488) were imaged and assayed (ImageJ, **D**). Source data for this figure is available on the online supplementary information page.

for the NF-treated PCI-15B cells with SAH and ~1 μM for the NF-treated HEK293 cells. Anti-EGFR-labeled NF was bound to PCI-15B at similar levels irrespective of SAH addition, and ~1.6-fold more than HEK293. Of note, DsRed fluorescence was highest on PCI-15B cells with SAH (Figures 5C and D). The number of DsRed-expressing bacteria bound to the PCI-15B cells was six times that of those bound to the HEK293 cells. In control experiments with no SAH which had no gradient in AI-2, there was neither a chemotactic response nor altered gene expression (<50 red fluorescing cells; Figures 5B–D). Importantly, the *in vitro* AI-2 quantified in 15B + SAH sample was 5 μM that was above the determined threshold for the QS switch (Supplementary Figure 1; Fernandes *et al*, 2010). Note that AI-2 has a dual role in both guiding bacterial chemotaxis and triggering the switching response (DsRed expression; Figure 5C). It was interesting, but unanticipated, that the threshold AI-2 level for *lsr* gene activation was nearly identical to that needed for cell motility.

Discussion

In summary, the docking of anti-EGFR-NF onto mammalian cell surfaces was specifically controlled by EGFR surface density which, in turn, controlled subsequent AI-2 synthesis, bacteria migration, and the switching response phenotype. The signal generating and cell recruiting design shown here provides a tractable means to ensure site-specific gene initiation, providing a focused and predicted phenotype. While we demonstrate signal transmission and bacterial homing in this system, a reduced system is feasible. For example, bacteria that naturally colonize specific niches could be re-wired to perform switching functions based on prevailing feature densities (e.g., Figures 3B and C) or localized cell number (via self-generated AI-2). As noted earlier, we have intentionally designed this system so that the incorporation of the control functions and output phenotype rely on minimally altered native circuits. This is in contrast to many applications of synthetic biology wherein artificial or metabolically orthogonal controllers (Gardner *et al*, 2000; Locke *et al*, 2011), pathways (Ro *et al*, 2006; Fortin *et al*, 2007; Atsumi *et al*, 2008; Dellomonaco *et al*, 2011), and functions (Elowitz and Leibler, 2000; Fung *et al*, 2005; Wong *et al*, 2007; Hsia *et al*, 2012) are transformed into cells yielding distinctly non-native cell behavior. That is, synthetic biology is replete with examples of novel biological tools (Stephanopoulos, 2002; Zhang *et al*, 2002; Warner *et al*, 2010) that endow cells with extraordinary biosynthetic capabilities (Ro *et al*, 2006; Fortin *et al*, 2007; Atsumi *et al*, 2008; Dellomonaco *et al*, 2011), tolerances (Patnaik *et al*, 2002; Stephanopoulos, 2002; Yang *et al*, 2010), and sense and respond phenotypes (Levskaya *et al*, 2005; Stricker *et al*, 2008). Often, in such cases, although individual cell productivity remains susceptible to stochastic diversity (Balazsi *et al*, 2011), cell populations are designed for and also 'aligned' for optimal production.

In the current work, we envision applications wherein the native QS systems already exist (e.g., GI tract), and Nature's cues feedback on and co-regulate the engineered bacterium (Anderson *et al*, 2006; Duan and March, 2010; Saeidi *et al*, 2011). In this way, the bacterium or a small sub-population of like cells, perform functions based on the prevailing conditions. In the system described here, the autoinducer guides both the bacterial motility and gene expression. While we have not engineered motility to respond to different AI-2 gradients, we have engineered cells that actuate gene expression based on different AI-2 concentrations. Perhaps, a single bacterium could be engineered so that chemotaxis and gene expression could be actuated by different concentrations of AI-2. As noted above, we also envision these phenotypes could be completely decoupled, using different signal molecules. We have also noted that motility responds in time domains far more rapidly than gene expression. Hence, the system could be tuned to operate based primarily on time rather than concentration so that distance traveled and gene expression are tuned for a desired function. Finally, while autonomous high-order functioning bacterial cells described here could be added to the growing arsenal of disease fighting bacteria (Forbes, 2006; Mengesha *et al*, 2007; St Stritzker *et al*, 2007; Jean *et al*, 2008; Duan and March, 2010; Patyar *et al*, 2010; Saeidi *et al*, 2011; Yu, 2011), we envision many applications wherein bacterial cells are engineered to carry out specified tasks.

Materials and methods

Cell strains and plasmid construction

E. coli K-12 W3110 (Δ*lsrFG* Δ*luxS*) was generated using a one-step inactivation method (Datsenko and Wanner, 2000) and were used throughout unless otherwise specified. This strain responds to a significantly lower AI-2 concentration than wild-type W3110 (Supplementary Figure 1). PCI-15B (Thomas *et al*, 2004) (provided by Dr Jennifer Grandis, University of Pittsburgh) is a cancer cell line that expresses EGFR at high levels. The EGFR displayed on the surface of PCI-15B enable bacterial targeting. HEK293 (human embryonic kidney cell, ATCC # CRL-1573) was used as control cells as they exhibit significantly lower EGFR on their surfaces. Both PCI-15B and HEK293 cells were cultivated in Dulbecco's Modified Eagle's Media (DMEM) containing glucose (4.5 g/l), GlutMAX I (3.97 mM), and 10% fetal bovine serum (FBS, Sigma) at 37°C with 5% CO_2. To construct the plasmid pET-DsRed_tac-ompA-proteinG (Supplementary Figure 2A), which encodes DsRed and surface displayed protein G, we performed PCR to amplify the surface display fragment including the outer membrane protein A and signal-peptide (lpp-ompA) sequences from the template vector, pTX101 (provided by Dr George Georgiou, University of Texas, Austin) (Francisco *et al*, 1992) and a protein G fragment, from pET32-E72G3 (provided by Dr Eiry Kobataki) (Tanaka *et al*, 2006). Subsequently, a fusion of lpp-ompA and a protein G gene fragment containing a *Hin*dIII site was generated again by PCR and then inserted into pET-DsRed with *Hin*dIII (NEB) ligation. The resulting plasmid product was then co-transformed along with pCT6 (Tsao *et al*, 2010) vector into W3110 (Δ*lsrFG* Δ*luxS*).

Bacteria response to *in vitro* AI-2 production

For creating differential antigen surface densities, various concentrations of avidin (Rockland Immunochemicals) were added to pre-treated biotin-coated plates (Pierce). Anti-avidin (FITC) conjugated NFs with 1:2 molar ratio (1/200 × dilution) were applied to guide the NF targeting toward the avidin surface. Bacteria, as described above, were resuspended in Dulbecco's Phosphate Buffer (DPBS; Sigma) containing 1 mM SAH (Sigma) and then incubated in the NF-treated plates. Bacterial responses to AI-2 production were monitored via their fluorescence response using a plate reader (SpectraMax M2; Molecular Devices). *In vitro* AI-2 levels were measured via a stoichiometric proxy, homocysteine, with the Ellman's assay.

In vitro bacteria targeting and switching/actuating

E. coli cells were induced with 0.5 mM IPTG for 2 h to express protein G followed by AF488-labeled mouse anti-EGFR (Santa Cruz Biotechnology) coupling. Bacterial cells were then applied to a 96-well plate (Greiner Bio-One) cultivated with PCI-15B and HEK293 cells for EGFR targeting. The wells were washed with DPBS to rinse off unbound bacteria and then treated with goat anti-mouse coupled NFs. After washing with DPBS, an SAH solution was added to the wells and bacterial fluorescence response was assessed over 12 h.

Simulation of *in vitro* AI-2 diffusion profile in the transwell configuration

The time-dependent AI-2 concentration distribution was modeled spatially utilizing COMSOL Multiphysics (COMSOL). Using an axis symmetric COMSOL model with the approximate dimensions of the transwell setup (BD Biosciences) and no flux across any boundaries, simulations were run to ensure that the AI-2 gradient across the transwell membrane persisted throughout the experimental time course. Diffusion was estimated to be 6×10^{-6} (cm^2/s) from the Wilke-Chang correlation with water as the solvent.

Chemotaxis due to *in vitro* synthesized AI-2

In vitro AI-2, SAH, and homocysteine (Sigma) were diluted into equivalent concentrations (40 μM) with DPBS and then added into the top compartment of transwells (3 μm porosity; BD Biosciences) in 6-well plates (Corning). *E coli* cells resuspended in DPBS (OD_{600} ~0.15) were then applied gently into the bottom compartment of the transwells. The plates were then incubated statically at 37°C for 2 h; bacterial dirigible density (OD_{600}) in the top compartment was assessed as a marker of cell motility.

Chemotaxis and QS-initiated gene expression in response to *in situ* AI-2 produced by locally targeted NFs

PCI-15B and HEK293 cells were seeded onto gelatin-treated glass slides (22 mm round; Fisher Scientific) 1 day before experiments. NF was coupled to anti-EGFR for 30 min incubation (2:1 molar ratio) and then diluted into 1% BSA-DPBS. Afterward, the cells were treated with anti-EGFR-NF for 0.5 h followed by rinsing with DPBS 3× and placed upside-down into 500 mM SAH (DPBS) containing transwells (3 μm porosity; 6-well plate formats). The glass slides were incubated at 37°C (in 5% CO_2) followed by the addition of bacteria (OD_{600} ~0.15 in DPBS) into the bottom compartment for a 9-h incubation. AI-2 production, bacterial migration, and genetic responses were examined by Ellman's assay, OD_{600}, and fluorescence microscopy, respectively.

Supplementary information

Supplementary information is available at the *Molecular Systems Biology* website (www.nature.com/msb).

Acknowledgements

We would like to thank Dr Jennifer Grandis for generously providing the PCI-15B cell line, Dr George Georgiou for kindly providing the *ompA* surface display vector, and Dr Eiry Kobatake for providing the *Streptococcal* protein G vector. This research was funded by the Defense Threat Reduction Agency (DTRA, BO085PO008), the Office of Naval Research (N000141010446), the National Science Foundation (EFRI-0735987) and the R.W. Deutsch Foundation.

Author contributions: H-CW, C-YT, DNQ, YC, KKC, GWR, GFP, JJV, and WEB conceived of the concepts, planned and designed the experiments. H-CW, C-YT, DNQ, MDS, YC, KKC, KJJ, JLT, and AZ performed the experiments and data analyses. H-CW, C-YT, DNQ, KKC, YC, and WEB wrote and edited the manuscript.

Conflict of interest

The authors declare that they have no conflict of interest.

References

Anderson JC, Clarke EJ, Arkin AP, Voigt CA (2006) Environmentally controlled invasion of cancer cells by engineered bacteria. *J Mol Biol* **355:** 619–627

Atsumi S, Hanai T, Liao JC (2008) Non-fermentative pathways for synthesis of branched-chain higher alcohols as biofuels. *Nature* **451:** 86–89

Balazsi G, van Oudenaarden A, Collins JJ (2011) Cellular decision making and biological noise: from microbes to mammals. *Cell* **144:** 910–925

Bentley WE, Mirjalili N, Andersen DC, Davis RH, Kompala DS (1990) Plasmid-encoded protein: the principal factor in the "metabolic burden" associated with recombinant bacteria. *Biotechnol Bioeng* **35:** 668–681

Carnes EC, Lopez DM, Donegan NP, Cheung A, Gresham H, Timmins GS, Brinker CJ (2010) Confinement-induced quorum sensing of individual Staphylococcus aureus bacteria. *Nat Chem Biol* **6:** 41–45

Datsenko KA, Wanner BL (2000) One-step inactivation of chromosomal genes in Escherichia coli K-12 using PCR products. *Proc Natl Acad Sci USA* **97:** 6640–6645

Defoirdt T (2011) Can bacteria actively search to join groups? *ISME J* **5:** 569–570

DeLisa MP, Valdes JJ, Bentley WE (2001) Quorum signaling via AI-2 communicates the 'Metabolic Burden' associated with heterologous protein production in Escherichia coli. *Biotechnol Bioeng* **75:** 439–450

Dellomonaco C, Clomburg JM, Miller EN, Gonzalez R (2011) Engineered reversal of the beta-oxidation cycle for the synthesis of fuels and chemicals. *Nature* **476:** 355–359

Duan F, March JC (2010) Engineered bacterial communication prevents Vibrio cholerae virulence in an infant mouse model. *Proc Natl Acad Sci USA* **107:** 11260–11264

Elowitz MB, Leibler S (2000) A synthetic oscillatory network of transcriptional regulators. *Nature* **403:** 335–338

Fernandes R, Roy V, Wu HC, Bentley WE (2010) Engineered biological nanofactories trigger quorum sensing response in targeted bacteria. *Nat Nanotechnol* **5:** 213–217

Fernandes R, Zuniga M, Sassine FR, Karakoy M, Gracias DH (2011) Enabling cargo-carrying bacteria via surface attachment and triggered release. *Small* **7:** 588–592

Forbes NS (2006) Profile of a bacterial tumor killer. *Nat Biotechnol* **24:** 1484–1485

Forbes NS (2010) Engineering the perfect (bacterial) cancer therapy. *Nat Rev Cancer* **10:** 785–794

Fortin PD, Walsh CT, Magarvey NA (2007) A transglutaminase homologue as a condensation catalyst in antibiotic assembly lines. *Nature* **448:** 824–827

Francisco JA, Earhart CF, Georgiou G (1992) Transport and anchoring of beta-lactamase to the external surface of Escherichia coli. *Proc Natl Acad Sci USA* **89:** 2713–2717

Fung E, Wong WW, Suen JK, Bulter T, Lee SG, Liao JC (2005) A synthetic gene-metabolic oscillator. *Nature* **435:** 118–122

Gardner TS, Cantor CR, Collins JJ (2000) Construction of a genetic toggle switch in Escherichia coli. *Nature* **403:** 339–342

Hegde M, Englert DL, Schrock S, Cohn WB, Vogt C, Wood TK, Manson MD, Jayaraman A (2011) Chemotaxis to the quorum-sensing signal AI-2 requires the Tsr chemoreceptor and the periplasmic LsrB AI-2-binding protein. *J Bacteriol* **193:** 768–773

Hooshangi S, Bentley WE (2008) From unicellular properties to multicellular behavior: bacteria quorum sensing circuitry and applications. *Curr Opin Biotechnol* **19:** 550–555

Hooshangi S, Bentley WE (2011) LsrR quorum sensing 'switch' is revealed by a bottom-up approach. *PLoS Comput Biol* **7:** e1002172

Hsia J, Holtz WJ, Huang DC, Arcak M, Maharbiz MM (2012) A feedback quenched oscillator produces turing patterning with one diffuser. *PLoS Comput Biol* **8:** e1002331

Kwok R (2010) Five hard truths for synthetic biology. *Nature* **463:** 288–290

Levskaya A, Chevalier AA, Tabor JJ, Simpson ZB, Lavery LA, Levy M, Davidson EA, Scouras A, Ellington AD, Marcotte EM, Voigt CA (2005) Synthetic biology: engineering Escherichia coli to see light. *Nature* **438:** 441–442

Locke JC, Young JW, Fontes M, Hernandez Jimenez MJ, Elowitz MB (2011) Stochastic pulse regulation in bacterial stress response. *Science* **334:** 366–369

Mengesha A, Dubois L, Chiu RK, Paesmans K, Wouters BG, Lambin P, Theys J (2007) Potential and limitations of bacterial-mediated cancer therapy. *Front Biosci* **12:** 3880–3891

Miller MB, Bassler BL (2001) Quorum sensing in bacteria. *Annu Rev Microbiol* **55:** 165–199

Patnaik R, Louie S, Gavrilovic V, Perry K, Stemmer WP, Ryan CM, del Cardayre S (2002) Genome shuffling of Lactobacillus for improved acid tolerance. *Nat Biotechnol* **20:** 707–712

Patyar S, Joshi R, Byrav DS, Prakash A, Medhi B, Das BK (2010) Bacteria in cancer therapy: a novel experimental strategy. *J Biomed Sci* **17:** 21

Ro DK, Paradise EM, Ouellet M, Fisher KJ, Newman KL, Ndungu JM, Ho KA, Eachus RA, Ham TS, Kirby J, Chang MC, Withers ST, Shiba Y, Sarpong R, Keasling JD (2006) Production of the antimalarial drug precursor artemisinic acid in engineered yeast. *Nature* **440:** 940–943

Saeidi N, Wong CK, Lo TM, Nguyen HX, Ling H, Leong SS, Poh CL, Chang MW (2011) Engineering microbes to sense and eradicate Pseudomonas aeruginosa, a human pathogen. *Mol Syst Biol* **7:** 521

Sahu N, Grandis JR (2011) New advances in molecular approaches to head and neck squamous cell carcinoma. *Anticancer Drugs* **22:** 656–664

St Jean AT, Zhang M, Forbes NS (2008) Bacterial therapies: completing the cancer treatment toolbox. *Curr Opin Biotechnol* **19:** 511–517

Stephanopoulos G (2002) Metabolic engineering by genome shuffling. *Nat Biotechnol* **20:** 666–668

Stricker J, Cookson S, Bennett MR, Mather WH, Tsimring LS, Hasty J (2008) A fast, robust and tunable synthetic gene oscillator. *Nature* **456:** 516–519

Stritzker J, Weibel S, Hill PJ, Oelschlaeger TA, Goebel W, Szalay AA (2007) Tumor-specific colonization, tissue distribution, and gene induction by probiotic Escherichia coli Nissle 1917 in live mice. *Int J Med Microbiol* **297:** 151–162

Tanaka G, Funabashi H, Mie M, Kobatake E (2006) Fabrication of an antibody microwell array with self-adhering antibody binding protein. *Anal Biochem* **350:** 298–303

Thomas SM, Zeng Q, Epperly MW, Gooding WE, Pastan I, Wang QC, Greenberger J, Grandis JR (2004) Abrogation of head and neck squamous cell carcinoma growth by epidermal growth factor receptor ligand fused to pseudomonas exotoxin transforming growth factor alpha-PE38. *Clin Cancer Res* **10:** 7079–7087

Tsao CY, Hooshangi S, Wu HC, Valdes JJ, Bentley WE (2010) Autonomous induction of recombinant proteins by minimally rewiring native quorum sensing regulon of E. coli. *Metab Eng* **12:** 291–297

Warner JR, Reeder PJ, Karimpour-Fard A, Woodruff LB, Gill RT (2010) Rapid profiling of a microbial genome using mixtures of barcoded oligonucleotides. *Nat Biotechnol* **28:** 856–862

Waters CM, Bassler BL (2005) Quorum sensing: cell-to-cell communication in bacteria. *Annu Rev Cell Dev Biol* **21:** 319–346

Wheeler DL, Dunn EF, Harari PM (2010) Understanding resistance to EGFR inhibitors-impact on future treatment strategies. *Nat Rev Clin Oncol* **7:** 493–507

Wong WW, Tsai TY, Liao JC (2007) Single-cell zeroth-order protein degradation enhances the robustness of synthetic oscillator. *Mol Syst Biol* **3:** 130

Xie Z, Wroblewska L, Prochazka L, Weiss R, Benenson Y (2011) Multi-input RNAi-based logic circuit for identification of specific cancer cells. *Science* **333:** 1307–1311

Yang S, Land ML, Klingeman DM, Pelletier DA, Lu TY, Martin SL, Guo HB, Smith JC, Brown SD (2010) Paradigm for industrial strain improvement identifies sodium acetate tolerance loci in Zymomonas mobilis and Saccharomyces cerevisiae. *Proc Natl Acad Sci USA* **107:** 10395–10400

Yu H (2011) Bacteria-mediated disease therapy. *Appl Microbiol Biotechnol* **92:** 1107–1113

Zhang YX, Perry K, Vinci VA, Powell K, Stemmer WP, del Cardayre SB (2002) Genome shuffling leads to rapid phenotypic improvement in bacteria. *Nature* **415:** 644–646

Zimmermann M, Zouhair A, Azria D, Ozsahin M (2006) The epidermal growth factor receptor (EGFR) in head and neck cancer: its role and treatment implications. *Radiat Oncol* **1:** 11

